A climatic evaluation of the southern dispersal route

Samuel L Nicholson[1,1], Rob Hosfield[2,2], Huw S Groucutt[3,3], Alistair W G Pike[4,4], Stephen J Burns[5,5], Albert Matter[6,6], and Dominik Fleitmann[2,2]

[1]Ecology and Evolutionary Biology, University of Reading, Reading, RG6 6LA, United Kingdom
[2]Department of Archaeology, University of Reading, Reading, RG6 6AB, United Kingdom
[3]Extreme Events Research Group, Max Planck Institute for Chemical Ecology, 07745 Jena, Jena, Germany
[4]Department of Archaeology, University of Southampton, Southampton, SO17 1BF, United Kingdom
[5]Department of Geosciences, University of Massachusetts, MA 01003-9297, United States of America
[6]University of Bern

December 1, 2022

Abstract

Homo sapiens dispersals out of Africa are often linked to intensifications of the African Summer Monsoon and Indian Summer Monsoon. Current dispersal models advocate that dispersals along the "southern-route" into Arabia occurred during Glacial Termination-II (T-II), when reduced sea-level and Bab-al-Mandab width increased the likelihood of crossing. The precise phasing between sea-level and monsoon precipitation is thus key to assess the likelihood of a successful crossing or the behavioural and technological capacities that facilitated crossing. Based on a precisely-dated stalagmite record from Yemen we reveal a distinct phase-lag of several thousand years between sea-level rise and monsoon intensification. Pluvial conditions in Southern Arabia during MIS 5e lasted from ~127.7 to ~121.1 ka BP and occurred when sea-levels were already higher than at present. Based on our observations, we propose three models for the dispersal of H. sapiens which all have pertinent implications for our understanding of human technological and behavioural capacities during MIS 5e.

Supplementary file and extended methods to "A climatic evaluation of the southern dispersal route during MIS 5e".

Samuel. L. Nicholson[1,2], Rob Hosfield[2], Huw S. Groucutt[3,4,5], Alistair W. G. Pike[6], Stephen J. Burns[7], Albert Matter[8], and Dominik Fleitmann[2,9]

[1] Ecology and Evolutionary Biology, University of Reading, Reading, RG6 6LA, United Kingdom.

[2] Department of Archaeology, University of Reading, Reading, RG6 6AB, United Kingdom.

[3] Extreme Events Research Group, Max Planck Institute for Chemical Ecology, 07745 Jena, Jena, Germany.

[4] Department of Archaeology, Max Plank Institutes for Chemical Ecology, the Science of Human History, and Biogeochemsitry, 07745 Jena, Germany.

[5] Institute of Prehistoric Archaeology, University of Cologne, Cologne, 5093, Germany.

[6] Department of Archaeology, University of Southampton, Southampton, SO17 1BF, United Kingdom.

[7] Department of Geosciences, University of Massachusetts, MA 01003-9297, United States of America.

[8] Institute of Geophysics, University of Bern, CH-3012 Bern, Switzerland.

[9] Department of Environmental Sciences, University of Basel, CH-4056 Basel, Switzerland.

Y99 Age-Depth model

Data selection

Growth interval-I (GI-I) is the most recent period of stalagmite deposition recorded in stalagmite Y99 (Fleitmann et al., 2011; Nicholson et al., 2020). Previous ^{230}Th dating analyses have shown that the 15.3 cm (composite depth of two growth axes: Fig. S1) period of stalagmite deposition falls within the Last Interglacial (MIS 5e), with ages ranging 132-117 ka BP (Fleitmann et al., 2011; Nicholson et al., 2020). GI-I can be visually and isotopically distinguished from GI-II (MIS 7a) and GI-III (MIS 7e), which are separated by clear growth discontinuities (Fig. S1) and abrupt shifts in $\delta^{18}O_{ca}$ values (Nicholson et al., 2020).

For this study, we selected only the more recent ^{230}Th age determinations (Nicholson et al., 2020) obtained using a refined methodology, smaller chronological uncertainties and revised U and Th decay constants (Cheng et al., 2013). Prior to age-depth modelling, one age (Y99-E-5; Fig. S1) was removed from consideration. This sample was collected from the top of the stalagmite, in which there is evidence of condensation corrosion. Such corrosion can cause localised open-system behaviour through post-depositional mobilisation of U and Th (Borsato et al., 2003; Scholz et al., 2014; Bajo et al., 2016). Whereas post-depositional leaching of U can lead to older ages, re-precipitation of calcite or incorporation of Th can cause younger ages. While no major period of growth following MIS 5e is observed in Y99, other stalagmites from Mukallah Cave (Y97-4 and Y97-5) indicate that drips were activated during the subsequent wet phases of MIS 5c and the Holocene (Fleitmann et al., 2011; Nicholson et al., 2020). These increase the likelihood that any minor activations of the Y99 drip following MIS 5e may have altered U or Th in the corroded area of GI-I, as supported by the relatively high ^{232}Th content compared to the rest of our sample. Due to these uncertainties, we excluded Y99-E-5 from our analyses. We proceeded with six previously published ages (Nicholson et al., 2020).

Age-depth model

The age-depth model for Y99 was constructed using the StalAge algorithm. StalAge is a available for the statistical software package R (Scholz and Hoffmann, 2011). One benefit of Stalage is that it can be applied to datasets which include outliers, age inversions, hiatuses and large changes in growth rate. StalAge acts in a three-step process, which allows major and minor outliers and age inversions to be detected, and the uncertainty of potential outliers is increased using an iterative procedure. An age model and with 95%-confidence limits are calculated by a Monte-Carlo simulation, which fits an ensemble of straight lines to the age data (Scholz and Hoffmann, 2011). One age reversal (Y99-E-3) was detected both visually and by the algorithm; the reason for this age inversion is unknown. An expansion of the uncertainty did not resolve this age inversion and was thus discarded from our age-depth model. Overall, the Y99 GI-I age-depth model is based on five^{230}Th measurements, spanning 127.811 ± 0.626 ka BP to 121.739 ± 0.561 ka BP.

Fig. S1. ^{230}Th ages and growth axes for stable isotope sampling of Y99 GI-I.^{230}Th ages marked in blue were not incorporated into (or were removed as outliers) from the StalAge age-depth model. Stalagmite growth discontinuities are marked by "D" numbers (see Fleitmann et al. 2011 and Nicholson et al. 2020 for further details on Y99).

Fig. S2. StalAge age-depth model for the MIS 5e section of Y99. The central age model (blue line) and 95% confidence intervals (red lines). Depth is the composite depth of axis-1 and axis-2. ^{230}Th ages in black represent ages used to construct the age model. The ^{230}Th age marked in blue is an outlier for unknown reasons and was discarded from the age model. See Nicholson et al. (2020) for ^{230}Th dating isotope information.

Bab-al-Mandab Strait reconstruction

The southern dispersal route hypothesis suggests that *H. sapiens*crossed into Arabia via the Bab al Mandab Strait (Stringer, 2000; Mellars, 2006; Armitage et al., 2011; Rohling et al., 2013). With a current width of ˜26 km, the Bab-al-Mandab Strait likely represented a significant challenge to *Homo sapiens* dispersals along the southern route. Thus, hypotheses favouring this route propose that maritime dispersal occurred during punctuated sea-level low-stands between 150,00 to 50 ka BP (Armitage et al., 2011; Rohling et al., 2013), when the width of the (BaM_{width}) Strait was substantially reduced. Previous analysis of composite Globigerinoides ruber $\delta^{18}O$ values from Red Sea marine cores KL-09, KL-11 and MD92-1017 have been used to reconstruct relative sea-levels over the past 500 kyrs (Rohling et al., 2009; Grant et al., 2012, 2014). The narrow Strait limits water to flow into the Red Sea creating a basin isolation effect, meaning that – unlike ocean core sea-level reconstructions which are based on deep-sea $\delta^{18}O_{benthic}$ values – the Red Sea Relative Sea Level curve (RSL) is independent from temperature forcing and instead records residence times of water in the basin, which are based on evaporation rates as determined by sea-level. Additionally, isostatic effects were accounted for in the creation of the RSL curve (Rohling et al., 2009), allowing us to assess sea-levels which control the sill depth at the Bab-al-Mandab strait. The Red Sea Relative Sea-Level (RSL) curve has been tuned to the $\delta^{18}O_{G.\ ruber}$ curve of LC21 (Mediterranean), another record to which the basin isolation concept has been applied (Grant et al., 2012). The chronology of LC21 has been derived from correlations with the revised chronology of the Soreq Cave $\delta^{18}O$ stalagmite record for the last 150 kyrs, and includes the chronology of the Sanbao Cave $\delta^{18}O$ stalagmite records and KL09 Ca/Ti up to 500 ka BP (Grant et al., 2012, 2014). Thus, the RSL is an excellent record for studying sea-level variation in the Red Sea. We therefore use the RSL curve and freely available elevation and bathymetry data at 15 arc-second interval resolution (˜450 metres at 14°N) (GEBCO Compilation Group, 2020) to reconstruct BaM_{width}over the past 150 kyrs.

We measured the minimum distance between contour lines at 10 m intervals between 20 to -120 m amsl on both sides of the strait using a variable-point method. Unlike a straight-point method, in which distances between equal contour lines are measured across a straight point A to point B transect, a variable-point method takes into consideration that the minimum width of the Strait shifted in space (Fig. S3). The variable model therefore provides an approximation of minimum possible crossing distances for *H. sapiens* in the Bab-al-Mandab area. We do not include islands in our analysis, until they are connected to the greater African and Arabian landmasses. While islands may have provided benefits to maritime crossings (i.e., breaking the crossing into smaller journeys), our method provides a record of the minimum distance of a crossing achieved in one journey.

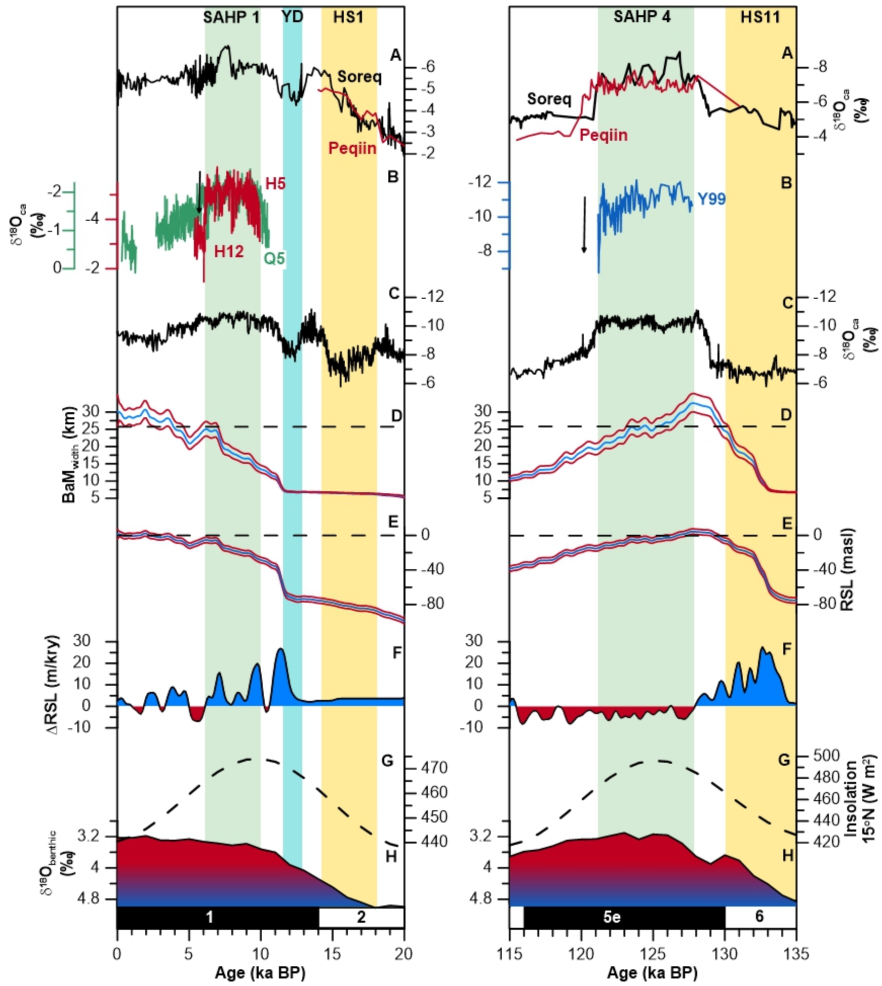

Fig. S3 . Elevation map showing variation of the minimum BaM_{width} (red line) under different sea-level scenarios. Pink lines denote contours at specified elevation/bathymetry.

Once depth-width data had been collected, we used an ensemble of polynomial fits to create a smooth model for width under different sea-level conditions. The final polynomial model was selected based on three criteria: 1) no width-depth inversions were detected (i.e., with increased depth, BaM_{width} must decrease); 2) a p-value of <0.05 and R^2 value >0.95 was achieved; and 3) our current measured width of the Strait (25.6 ± 0.225 km) must fall within the 95% confidence intervals of the polynomial model. We chose a 3-order polynomial fit. While 4-6 order fits provided higher R^2 values, these resulted in substantial width-depth inversions (i.e., as sea-levels decreased, at points BaM_{width} increased) when combined with the RSL. The resultant formula of the fit (Fig. S4A) was combined with the RSL Probability Maximum curve and 95% confidence intervals (Grant et al., 2012, 2014) to provide models for the minimum BaM_{width}at 0.125 kyr intervals over the last 130 ka BP. Our modelled BaM_{width} at 0 ka BP (30.15 +4.88/-4.26 km) is slightly greater than our measured width (25.6 ± 0.225 km). (fig. 4). We relate this to two complications: 1) the complex elevation and bathymetry of the Bab-al-Mandab area (sudden changes in elevation gradients) which the smooth polynomial fit does not easily detect (Fig. S4A), and 2) the RSL slightly overpredicts present sea-levels by ~1.7 m. However, uncertainties of the measured width (25.6 ± 0.225 km) and modelled width (30.15 +4.88/-4.26 km) overlap, and the measured width falls within the 95% confidence intervals of the polynomial fit. Additionally, the chosen polynomial fit slightly underestimates contour distance at +10 m, meaning that the reconstructed BaM_{width} is slightly conservative to sea-level increases during early MIS 5e.

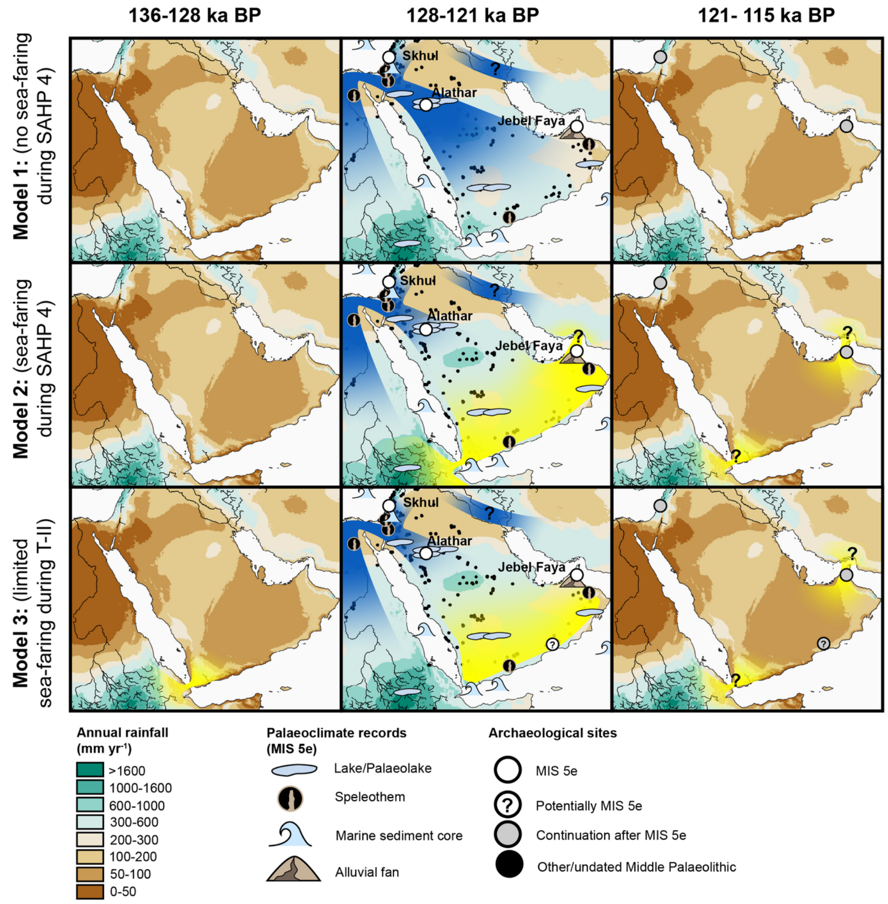

Fig. S4. A) Contour height and minimum distance between contours of the Bab-al-Mandab Strait plotted with the 3rd order polynomial fit (blue line) and 95% confidence intervals using 5000 iterations (red shaded area and lines). The arrow shows our 0 m contour and measured current $\mathrm{BaM}_{\mathrm{width}}$. Formula and model coefficients are given below. B) Modelled $\mathrm{BaM}_{\mathrm{width}}$ over the last 150 kyrs using the RSL P-max (blue line) and the RSL P-max 95% confidence intervals (red lines).

References

Armitage, S.J., Jasim, S.A., Marks, A.E., Parker, A.G., Usik, V.I., Uerpmann, H.P., 2011. The southern route “out of Africa”: Evidence for an early expansion of modern humans into Arabia. Science. 331, 453–456.

Bajo, P., Hellstrom, J., Frisia, S., Drysdale, R., Black, J., Woodhead, J., Borsato, A., Zanchetta, G., Wallace, M.W., Regattieri, E., Haese, R., 2016. “Cryptic” diagenesis and its implications for speleothem geochronologies. Quaternary Science Reviews. 148, 17–28.

Borsato, A., Quinif, Y., Bini, A., Dublyansky, Y. V., 2003. Open-system alpine speleothems: implications for U-series dating and palaeoclimate reconstructions. Studi Trentini di Scienze Naturali – Acta Geologica. 80, 71–83.

Cheng, H., Lawrence Edwards, R., Shen, C.C., Polyak, V.J., Asmerom, Y., Woodhead, J., Hellstrom, J., Wang, Y., Kong, X., Spötl, C., Wang, X., Calvin Alexander, E., 2013. Improvements in ^{230}Th dating, ^{230}Th and ^{234}U half-life values, and U-Th isotopic measurements by multi-collector inductively coupled plasma mass spectrometry. Earth and Planetary Science Letters. 371–372, 82–91.

Fleitmann, D., Burns, S.J., Pekala, M., Mangini, A., Al-Subbary, A., Al-Aowah, M., Kramers, J., Matter, A., 2011. Holocene and Pleistocene pluvial periods in Yemen, southern Arabia. Quaternary Science Reviews. 30, 783–787.

GEBCO Compilation Group, 2020. GEBCO 2020 Grid.

Grant, K.M., Rohling, E.J., Bar-Matthews, M., Ayalon, A., Medina-Elizalde, M., Ramsey, C.B., Satow, C., Roberts, A.P., 2012. Rapid coupling between ice volume and polar temperature over the past 50,000 years. Nature. 491, 744–747.

Grant, K.M., Rohling, E.J., Ramsey, C.B., Cheng, H., Edwards, R.L., Florindo, F., Heslop, D., Marra, F., Roberts, A.P., Tamisiea, M.E., Williams, F., 2014. Sea-level variability over five glacial cycles. Nature Communications. 5, 5076.

Mellars, P., 2006. Why did modern human populations disperse from Africa ca. 60,000 years ago? A new model. Proceedings of the National Academy of Sciences. 103, 9381–9386.

Nicholson, S.L., Pike, A.W.G., Hosfield, R., Roberts, N., Sahy, D., Woodhead, J., Cheng, H., Edwards, R.L., Affolter, S., Leuenberger, M., Burns, S.J., Matter, A., Fleitmann, D., 2020. Pluvial periods in Southern Arabia over the last 1.1 million-years. Quaternary Science Reviews. 229, 106112.

Rohling, E.J., Grant, K., Bolshaw, M., Roberts, A.P., Siddall, M., Hemleben, C., Kucera, M., 2009. Antarctic temperature and global sea level closely coupled over the past five glacial cycles. Nature Geoscience. 2, 500–504.

Rohling, E.J., Grant, K.M., Roberts, A.P., Larrasoaña, J.-C., 2013. Paleoclimate Variability in the Mediterranean and Red Sea Regions during the Last 500,000 Years. Current Anthropology. 54, S183–S201.

Scholz, D., Hoffmann, D.L., 2011. StalAge - An algorithm designed for construction of speleothem age models. Quaternary Geochronology. 6, 369–382.

Scholz, D., Hoffmann, D.L., Jochum, K.P., Spötl, C., Riechelmann, D.F.C., 2014. Diagenesis of speleothems and its effects on the accuracy of 230Th/U-ages. Chemical Geology. 387, 74–86.

Stringer, C., 2000. Coasting out of Africa. Nature. 405, 24–27.

A climatic evaluation of the southern dispersal route during MIS 5e.

Samuel L. Nicholson[1,2], Rob Hosfield[2], Huw S. Groucutt[3,4,5], Alistair W. G. Pike[6], Stephen J. Burns[7], Albert Matter[8], and Dominik Fleitmann[2,9]

[1] Ecology and Evolutionary Biology, University of Reading, Reading, RG6 6LA, United Kingdom.

[2] Department of Archaeology, University of Reading, Reading, RG6 6AB, United Kingdom.

[3] Extreme Events Research Group, Max Planck Institute for Chemical Ecology, 07745 Jena, Jena, Germany.

[4] Department of Archaeology, Max Plank Institutes for Chemical Ecology, the Science of Human History, and Biogeochemsitry, 07745 Jena, Germany.

[5] Institute of Prehistoric Archaeology, University of Cologne, Cologne, 5093, Germany.

[6] Department of Archaeology, University of Southampton, Southampton, SO17 1BF, United Kingdom.

[7] Department of Geosciences, University of Massachusetts, MA 01003-9297, United States of America.

[8] Institute of Geophysics, University of Bern, CH-3012 Bern, Switzerland.

[9] Department of Environmental Sciences, University of Basel, CH-4056 Basel, Switzerland.

Corresponding authors: Samuel L. Nicholson (`sam.nicholson@reaeding.ac.uk`)

Dominik Fleitmann (`dominik.fleitmann@unibas.ch`)

Highlights:

- Timing of monsoon intensification in Arabia confined to 127.7 ka BP until 121.1 ka BP.
- Most substantial increase of rainfall in the last 130 ka BP.
- Onset of the pluvial period lagged sea-level rise.

Abstract

Homo sapiens dispersals out of Africa are often linked to intensifications of the African Summer Monsoon and Indian Summer Monsoon. Current dispersal models advocate that dispersals along the “southern-route” into Arabia occurred during Glacial Termination-II (T-II), when reduced sea-level and Bab-al-Mandab width increased the likelihood of crossing. The precise phasing between sea-level and monsoon precipitation is thus key to assess the likelihood of a successful crossing or the behavioural and technological capacities that facilitated crossing. Based on a precisely-dated stalagmite record from Yemen we reveal a distinct phase-lag of several thousand years between sea-level rise and monsoon

intensification. Pluvial conditions in Southern Arabia during MIS 5e lasted from ~127.7 to ~121.1 ka BP and occurred when sea-levels were already higher than at present. Based on our observations, we propose three models for the dispersal of *H. sapiens* which all have pertinent implications for our understanding of human technological and behavioural capacities during MIS 5e.

1 Introduction

Understanding how *H. sapiens* spread from Africa across the world is one of the most debated topics in human evolution (Mellars et al., 2013; Groucutt et al., 2015a; Bae et al., 2017). Two proposed main dispersal routes cross Arabia: a northern-route across the Sinai into the Levant and a southern-route from the Horn of Africa via the Strait of Bab-al-Mandab into Southern Arabia and beyond (Fig. 1). The accessibility of these entry points was spatiotemporally variable and related to major climatic changes across the Saharo-Arabian deserts. During interglacial periods, both the African and Indian Summer Monsoons (ASM and ISM, respectively) were much stronger, expanded northward and transformed the Saharo-Arabian deserts into green landscapes for a few millennia (Fleitmann et al., 2003b; Parton et al., 2015; Petraglia et al., 2015; Tierney et al., 2017; Nicholson et al., 2020). These pluvial periods, termed "Green Arabia Periods" and "South Arabian Humid Periods" (SAHPs) respectively, provided optimal periods for *H. sapiens* to disperse from sub-Saharan Africa into Eurasia (Fleitmann et al., 2011; Rosenberg et al., 2011; Larrasoaña et al., 2013; Nicholson et al., 2020). Over the last 130 ka BP, pluvial conditions in Southern Arabia with rainfall of more than 300 mm yr^{-1} occurred during Marine Isotope Stages (MIS) 5 and 1, and lasted from ~128-121 ka BP (MIS 5e; SAHP 4), ~104-97 ka BP (MIS 5c; SAHP 3) and ~84-71 ka BP (MIS 5a; SAHP 2) and ~10.5 to 6.2 ka BP (SAHP 1) (Fleitmann et al., 2011; Nicholson et al., 2020). In addition, there is also some evidence for a period of enhanced rainfall between approximately 60 and 50 ka BP (the onset of MIS 3) (McLaren et al., 2009; Parton et al., 2013, 2018), though the nature and timing of this period remains uncertain.

The southern dispersal route involves a maritime crossing of the Bab-al-Mandab Strait. However, its current width of approximately ~26 km represents a significant challenge to dispersal and was more likely traversable at times of lower sea-level, especially if sea-faring technologies were limited. One proposed timing for early *H. sapiens* dispersals is Glacial Termination-II (T-II), between 136-129 ka BP, when sea-levels, although rapidly rising, were lower than today and the width of the Bab-al-Mandab Strait (BaM_{width}) was reduced to a few kilometres (Armitage et al., 2011). From a palaeoclimatic perspective, a dispersal was most likely to have occurred at times of increased precipitation and biomass across Arabia. However, during T-II, several lines of evidence point to a phase-lag of several thousand years between sea-level rise and northward migration of the tropical rainbelt due to colder northern-hemisphere temperatures related to Heinrich Stadial (HS) 11 between 135 and 130 ka BP (Cheng et al., 2009; Böhm et al., 2015; Häuselmann et al., 2015; Marino et al., 2015). In other words, arid conditions may have prevailed in Arabia during T-II, forming a biogeographical barrier to widespread dispersals despite low sea-levels. Thus, establishing the precise phasing between sea-level change and ASM/ISM intensification during the MIS 6-5e transition from records close to the Bab-al-Mandab Strait could be one critical factor for understanding accessibility of the southern-dispersal route. ASM and ISM records with precise and accurate chronologies are an important prerequisite to reveal such a phasing. Here, we present a precisely-dated and highly-resolved speleothem-based climate record from Mukalla Cave in Yemen, covering MIS 5e (SAHP 4: Nicholson et al., 2020). Precise Uranium-series (^{230}Th) ages allow us to evaluate the temporal phasing between ASM/ISM rainfall and sea-level change at a possible point of entry into southern Arabia.

2 Environmental Settings, materials and methods

Stalagmite Y99 was collected from Mukalla Cave (14°55’02’ ’N; 48°35’23’ ’ E; ~1500 masl; Fig. 1) in southern Yemen, where climate is strongly governed by the ASM and ISM respectively. At present, both Mukalla Cave and the Bab-al-Mandab Strait are located at the northern and north-eastern margins of the ASM and ISM, with rainfall averaging <150 mm yr^{-1} (Fleitmann et al., 2011). Stalagmite Y99 extends back to 1.1 million years and was deposited in 17 punctuated growth intervals identified through ^{230}Th and Uranium-lead dating, with Growth Interval-I (GI-I) being the youngest and dated to MIS 5e (Nicholson et al., 2020). Previously analysis of Y99 was focussed on the broad timing and climatic conditions (bulked ^{18}O and ^{13}C isotope analysis) of SAHPs over the last 1.1 million-years (Fleitmann et al., 2011; Nicholson et al., 2020). Here, we provide a more high-resolution and focussed study of the timing of SAHP 4 compared to sea-level fluctuation. We used the StalAge algorithm to produce a robust age-model for SAHP 4 from previously collected ^{230}Th ages. This was then used to provide $^{18}O_{ca}$ (ASM rainfall) and $^{13}C_{ca}$ records at <100 years resolution and can be accurately compared to sea-level records.

The width of the Bab-al-Mandab Strait (BaM_{width}) was reconstructed using bathymetry data and the Red Sea relative sea-level (RSL) curve. The RSL has been constructed using marine core $^{18}O_{G.\ ruber}$ records from the Red Sea (Siddall et al., 2003; Rohling et al., 2009), whereas the chronology of the RSL time-series is based on correlations with Mediterranean Core LC21 and the revised ^{230}Th chronology of the Soreq Cave record for periods younger than 150 ka BP (Rohling et al., 2009; Grant et al., 2012, 2014). Using local sea-level records that exploit a basin isolation effect means that our assessment is unaffected by isostatic effects, allowing us to compare regional climates with sea-level variations that control the sill depth and the width of the Strait. We used the freely available QGIS software package and 15 arc-second (~450 m between 12-14°N) interval elevation and bathymetry data (GEBCO Compilation Group, 2020) in combination with the RSL to estimate BaM_{width} over the last 150 kyrs (extended methods).

3 Results and discussion

3.1 Timing and Duration of SAHP 4 (MIS 5e)

The chronology of the MIS 5e section of stalagmite Y99 is based on seven ^{230}Th ages. Two ages were discarded: one ^{230}Th age at the top was not included as it is most likely influenced by condensation corrosion and one age appears to be an outlier for unknown reasons (Extended methods; Fig. S1 and S2). Importantly, the onset of stalagmite growth is determined by two ^{230}Th ages of 127.634 ± 0.557 ka BP and 127.811 ± 0.626 ka BP; whereas the StalAge model places the onset of growth at 127.725 +/- 0.448/0.374 ka BP. Stalagmite growth ceased at around 121.170 ± 0.500 ka BP (Fig. 2A). As ~300 mm yr^{-1} of rainfall are mostly likely required to trigger large speleothem growth in desert caves (Vaks et al., 2010), onset of stalagmite growth reveals that monsoonal rainfall during MIS 5e (SAHP 4) was at least twice as high as today. Considering the height and diameter of stalagmite Y99 and contemporaneously deposited speleothems in Hoti Cave in Northern Oman (Burns et al., 2001; Fleitmann et al., 2011), ASM and ISM rainfall must have been considerably higher than 300 mm yr^{-1} (Burns et al., 2001). This assumption is also supported by model-based estimates of rainfall over Arabia during MIS 5e (Otto-Bliesner, 2006; Herold and Lohmann, 2009; Jennings et al., 2015; Gierz et al., 2017). Based on the age model for stalagmite Y99, SAHP 4 lasted for ~6.5 kyrs, which is slightly longer than the 4.3 kyr-long Holocene Humid period in Southern Arabia (Fleitmann et al., 2007) (Fig. 3).

Additional evidences support the timing and duration of SAHP 4. The onset of the MIS 5e growth interval (SAHP 4) of stalagmite Y99 at 127.725 +/- 0.448/0.374 ka BP is synchronous with the onset of sapropel S5 at ~128.3 ± 2 ka BP (Grant et al., 2017) and associated negative shifts in speleothem $^{18}O_{ca}$ records from Soreq and Peqiin Caves in Israel (Bar-Matthews et al., 2003). In both caves, speleothem $^{18}O_{ca}$ values are influenced by the "source effect" as ^{18}O of (palaeo)precipitation in the Levant is directly linked to ^{18}O of surface water in the Eastern Mediterranean. During interglacial periods, increased monsoon precipitation in the Ethiopian Highlands and higher discharge of low- ^{18}O freshwater runoff from the Nile and North African wadi systems (Grant et al., 2012) into the Mediterranean lead to more negative ^{18}O and sapropel formation (Rohling et al., 2015). Thus, the sharp decrease in $^{18}O_{ca}$ at ~128.3 ± 1.2 ka BP in the Soreq and Peqiin Cave records (Fig. 3) is caused by an up to ~8 times higher Nile flow (compared to the pre-Aswan period; Amies et al., 2019) during MIS 5e. Taken together, the Soreq and Peqiin Cave records are in line with marked increase in ASM and ISM rainfall at onset of SAHP 4 at 127.725 +/- 0.448/0.374 ka BP in stalagmite Y99, supporting the accuracy of its chronology. The termination of SAHP 4 at 121.170 ± 0.500 ka BP is also concurrent with the independently derived age estimate for the termination of sapropel S5 at ~121.5 ± 2 ka BP (Grant et al., 2016, 2017) and the distinct positive shift in $^{18}O_{ca}$ in the Soreq and Peqiin Cave records (Bar-Matthews et al., 2003). Such a close correspondence between sapropel deposition in the Eastern Mediterranean and the timing of peak rainfall in Southern Arabia is also observed for other SAHPs (Nicholson et al., 2020) and (SAHP 1) between 10.5 and 6.2 ka BP (Fleitmann et al., 2007; Grant et al., 2017). The timing of SAHP 4 also conforms with significantly higher ASM/ISM rainfall in other – albeit less precisely-dated – monsoon records (Weldeab et al., 2007; Grant et al., 2017; Tierney et al., 2017; Fig. 4).

3.2 Climatic and Environmental Conditions During SAHP 4

It has been shown that fluctuations in $^{18}O_{ca}$ from Mukalla Cave speleothems are related to changes in the amount of ASM precipitation in Yemen (Fleitmann et al., 2011; Nicholson et al., 2020). This is confirmed by isotope measurements (D and ^{18}O) of stalagmite fluid inclusion water, showing that the ASM was the dominant moisture source at Mukalla Cave during MIS 5e (Nicholson et al., 2020). The $^{18}O_{ca}$ profile of stalagmite Y99 shows three distinct features. Firstly, $^{18}O_{ca}$ values are lowest at onset and during the first phase of SAHP 4, indicating that ASM rainfall increased rapidly at the onset of SAHP 4, most likely within a few centuries and similar to ISM monsoon records (Fleitmann et al., 2003a). Secondly, ASM rainfall is highest until ~124 ka BP and decreases following summer insolation. Thirdly, the abrupt positive shift in $^{18}O_{ca}$ at 121.170 ± 0.500 ka BP indicates an abrupt termination of SAHP 4, most likely within a few decades (Burns et al., 2001). This is a common feature of SAHPs (Nicholson et al., 2020) and related to the geographical position of the cave in relation to the position of the Intertropical Convergence Zone and monsoonal rainfall belt respectively (Fleitmann et al., 2007). The abrupt termination of speleothem growth and positive shift indicates a rapid retraction of the Intertropical Convergence Zone and associated monsoonal rainfall southwards of Mukalla Cave. In addition, Y99 SAHP 4 $^{18}O_{ca}$ values show that monsoon precipitation was substantially higher during MIS 5e (SAHP 4) compared with subsequent SAHPs (Fig. 2B). This isotopic difference is also observed at Hoti Cave (Fleitmann et al., 2011; Nicholson et al., 2020) (Fig. 2B). Overall, Y99 $^{18}O_{ca}$ values indicate that MIS 5e saw the most substantial enhancement of monsoon precipitation during the Late Pleistocene.

Stalagmite Y99 $^{13}C_{ca}$ values are influenced by numerous factors, including vegetation type and density, and soil thickness and moisture above the cave (Nicholson et al., 2020). However, the various, and sometimes counteracting, controls means that stalagmite $^{13}C_{ca}$ values can be difficult to interpret and that the principal factors controlling $^{13}C_{ca}$ values may change over time. Y99 $^{13}C_{ca}$ values vary between -4.6 and -9.0 ‰ and thus fall into a mixed C_3/C_4 vegetation signal (Clark and Fritz, 1997), suggesting that grasslands with some woody cover were present above Mukalla Cave during SAHP 4. This is consistent with palaeontological records across Arabia and phytolith records from Jebel Faya (MIS 5e) and Mundafan (MIS 5c/5a), indicating that now arid areas of Arabia were characterised by grasslands and some woody cover during wetter periods (Rosenberg et al., 2011, 2013; Bretzke et al., 2013; Groucutt et al., 2015c; Stewart et al., 2020a, 2020b). Similar to the Y99 $^{18}O_{ca}$ profile, the termination of stalagmite growth is characterised by an abrupt increase in $^{13}C_{ca}$ (Fig. 2A) as rainfall, drip-rate and vegetation density decreased rapidly above Mukalla Cave. Overall, the Mukalla Cave $^{13}C_{ca}$ profile indicates that increased rainfall was associated with the formation of herbaceous grasslands, with some woody cover, in the now arid interior of Yemen during MIS 5e.

3.3 Phasing between pluvial conditions in Southern Arabia and sea-level change during MIS 5e

Based on the stalagmite Y99 stable isotope records, climatic and environmental conditions in Southern Arabia were generally favourable for human dispersal along the southern dispersal route during MIS 5e. A key-question is therefore whether BaM_{width} was narrow enough for a successful crossing into Arabia during MIS 5e and SAHP 4. The absolute and precise age-models for the MIS 5e (SAHP 4) growth interval of stalagmite Y99 allows the comparison of the phasing between monsoonal rainfall, the RSL and BaM_{width} (Fig. 3). The onset of SAHP 4 at 127.725 +/- 0.448/0.3741 ka BP occurred when global sea-level was already 4.7 ± 3.9 m higher than today and the width of the Bab-al-Mandab Strait was >26 km, similar or even wider than today. Furthermore, at the end of SAHP 4 (121.170 ± 0.500 ka BP), global sea level was only 14.7 ± 3.1 m lower than today, yet the Bab-al-Mandab was ~20 km wide and therefore remained a major obstacle to the southern dispersal route.

The observed time lag between sea-level rise and the onset of pluvial conditions in Arabia is consistent with a growing body of evidence for a decoupling of monsoon intensification and rising low-latitude insolation during T-II. Low-latitude insolation is a key control on the interhemispheric pressure gradient (iHPG), which regulates the intensity and position of the monsoon domain (e.g., Beck et al., 2018). Yet, despite rising insolation throughout T-II, our data, as well as previously published records from Sanbao (Cheng et al., 2009) and Soreq (Bar-Matthews et al., 2003; Grant et al., 2012, 2016; Häuselmann et al., 2015) caves, indicate that monsoon intensification did not occur until ~129-128 ka BP. This lag can be related to the effects of the cold northern hemisphere conditions during HS11 (135-130 ka BP). HS11 punctuated the warming of T-II and coincides with a major deglacial meltwater discharge (up to 0.3 Sv) phase into the North Atlantic (Marino et al., 2015). Meltwater discharge contributed to up to 70% of sea-level rise during T-II (Marino et al., 2015) and slowed, or maybe even led to a collapse of AMOC (Böhm et al., 2015) leading to colder northern hemisphere temperatures. This reduced the iHPG, suppressed the effects of rising insolation, and inhibited the migration of both the ASM/ISM and the EAM (Cheng et al., 2009; Häuselmann et al., 2015). Only once freshwater discharge and northern hemisphere temperatures stabilised ~128 ka BP (Marino et al., 2015) could insolation have a full effect on the iHPG and permitted northward migration of the monsoon rainbelt. Therefore, not only did high sea-levels act as a potential barrier to dispersal during MIS 5e, a supressed ASM/ISM throughout T-II meant that more arid conditions prevailed in Arabia and northeastern Africa when sea-levels were lower than today.

4 Models for *H. sapiens* dispersals across the southern-route

With a present-day minimum width of ~26 km, the Bab-al-Mandab would represent a major obstacle for *H. sapiens* dispersals. A common suggestion is that a reduced width of the Strait facilitated a maritime crossing during T-II (Armitage et al., 2011; Bae et al., 2017). However, the Y99 record indicates that the intensification of the monsoon lagged behind sea-level rise during T-II and instead occurred once $\mathrm{BaM}_{\mathrm{width}}$ had reached its Late Pleistocene maximum. This instead suggests that the most optimal period of *H. sapiens* dispersal, from a palaeoclimatic perspective, was between 128 and 121 ka BP, when increased rainfall transformed Southern Arabia into a grassland biome. The lag between sea-level rise and the onset of pluvial conditions has potentially important implications for understanding both the route of *H. sapiens* dispersals and also the cognitive, behavioural and technological capacities they possessed. Here, we provide three, not necessarily mutually exclusive, potential models for human dispersals throughout T-II and SAHP 4 (Fig. 4):

1. Dispersal occurred via a northern land-route during favourable conditions across Saharo-Arabia occurred between 128-121 ka BP and followed palaeohydrological corridors into Arabia and the Levant (Breeze et al., 2016; Nicholson et al., 2021).

2. A maritime dispersal via the southern-route occurred when sea-levels were high, but climates were favourable between 128-121 ka BP.

3. A maritime dispersal via the southern-route occurred prior to the onset of favourable climatic and environmental conditions, when sea-levels were low >128 ka BP (Armitage et al., 2011; Rohling et al., 2013).

Both model 2 and 3 require evidence of sea-faring, which is currently unknown prior to 60-50 ka BP (Norman et al., 2018), and model 3 assumes that *H. sapiens* were rather tolerant of arid and semi-arid conditions or exploited productive coastal environments (Erlandson and Braje, 2015). Previous findings, however, have linked occupations of the now Saharo-Arabian deserts interiors to wetter phases of MIS 5, providing support for model 1. This model is supported by the archaeological assemblages from northeast Africa, the Nafud Desert and the Levant; techno-cultural similarities suggest cultural exchange between these regions (Groucutt et al., 2015b, 2019).

The validity of the southern dispersal route hypothesis is therefore dependent on evidence of sea-faring prior to and during MIS 5e, which is currently absent between Africa and SE Asia, and/or flexible environmental tolerances of *H. sapiens*. Conversely, the northern-route into Arabia was a viable route throughout SAHP 4. Whether crossing the Bab-al-Mandab Strait was an additional route will require further archaeological investigation of coastal settings (e.g., Bailey et al., 2015) to establish clear demographic links between both sides of the Strait and providing examples of the sea-faring capabilities prior to 60 ka. Additionally, future dispersal pathway modelling studies must synthesise climatic, environmental and other topographic factors (e.g., Groucutt, 2020), which might have various and counteracting effects, to understand the variations of *H. sapiens* biogeographies.

5 Conclusions

Overall, our results indicate that the onset of increased rainfall occurred at 127.7 ka BP, after maximum deglaciation and sea-level rise. Whereas aridity prevailed throughout T-II when sea-levels were lower, the Bab-al-Mandab was at its greatest width at the onset of SAHP 4. We observe a distinct phase-lag between sea-level rise and monsoon intensification from records in close proximity to one-another. Our findings have pertinent impacts for understanding (1) the timing of monsoon intensification relative to sea-level rise throughout T-II in the Horn of Africa and Southern Arabia. (2) The timings and geographies of *H. sapiens* dispersals during MIS 5e, and (3) the potential behavioural and technological capabilities of *H. sapiens* at the onset of the Late Pleistocene.

Acknowledgments, Samples, and Data

This work was supported by the AHRC South, West and Wales Doctoral Training Partnership (Grant AH/L503939/1) the Swiss National Science Foundation (Grant PP002-110554/1 to DF). The initial stable-isotope and ^{230}Th age data used to construct the age-model is available at Nicholson et al. (2020). Our original StalAge age-depth data has been submitted to the data repository PANGAEA, which complies with FAIR principles. On acceptance of our manuscript our data will be made available at PANGAEA.

References

Amies, J.D., Rohling, E.J., Grant, K.M., Rodríguez-Sanz, L., Marino, G., 2019. Quantification of African Monsoon Runoff During Last Interglacial Sapropel S5. Paleoceanography and Paleoclimatology. 34, 1487–1516.Armitage, S.J., Jasim, S.A., Marks, A.E., Parker, A.G., Usik, V.I., Uerpmann, H.P., 2011. The southern route “out of Africa”: Evidence for an early expansion of modern humans into Arabia. Science. 331, 453–456.Bae, C.J., Douka, K., Petraglia, M.D., 2017. On the origin of modern humans: Asian perspectives. Science. 358, eaai9067.Bailey, G.N., Devès, M.H., Inglis, R.H., Meredith-Williams, M.G., Momber, G., Sakellariou, D., Sinclair, A.G.M., Rousakis, G., Al Ghamdi, S., Alsharekh, A.M., 2015. Blue Arabia: Palaeolithic and underwater survey in SW Saudi Arabia and the role of coasts in Pleistocene dispersals. Quaternary International. 382, 42–57.Bar-Matthews, M., Ayalon, A., Gilmour, M., Matthews, A., Hawkesworth, C.J., 2003. Sea - land oxygen isotopic relationships from planktonic foraminifera and speleothems in the Eastern Mediterranean region and their implication for paleorainfall during interglacial intervals. Geochimica et Cosmochimica Acta. 67, 3181–3199.Beck, J.W., Zhou, W., Li, C., Wu, Z., White, L., Xian, F., Kong, X., An, Z., 2018. A 550,000-year record of East Asian monsoon rainfall from 10Be in loess. Science. 360, 877–881.Berger, A., Loutre, M.F., 1991. Insolation values for the climate of the last 10 million years. Quaternary Science Reviews. 10, 297–317.Berger, A., Loutre, M.F., 1999. Parameters of the Earths orbit for the last 5 Million years in 1 kyr resolution. Supplement to: Berger, A; Loutre, M F (1991): Insolation values for the climate of the last 10 million of years. Quaternary Science Reviews, 10(4), 297-317, doi:10.1016/0277-3791(91)90033-Q.Böhm, E., Lippold, J., Gutjahr, M., Frank, M., Blaser, P., Antz, B., Fohlmeister, J., Frank, N., Andersen, M.B., Deininger, M., 2015. Strong and deep Atlantic meridional overturning circulation during the last glacial cycle. Nature. 517, 73–76.Breeze, P.S., Groucutt, H.S., Drake, N.A., White, T.S., Jennings, R.P., Petraglia, M.D., 2016. Palaeohydrological corridors for hominin dispersals in the Middle East ~250-70,000 years ago. Quaternary Science Reviews. 144, 155–185.Bretzke, K., Armitage, S.J., Parker, A.G., Walkington, H., Uerpmann, H.P., 2013. The environmental context of Paleolithic settlement at Jebel Faya, Emirate Sharjah, UAE. Quaternary International. 300, 83–93.Burns, S.J., Fleitmann, D., Matter, A., Neff, U., Mangini, A., 2001. Speleothem evidence from Oman for continental pluvial events during interglacial periods. Geology. 29, 623–626.Cheng, H., Edwards, R.L., Broecker, W.S., Denton, G.H., Kong, X., Wang, Y., Zhang, R., Wang, X., 2009. Ice age terminations. Science. 326, 248–252.Cheng, H., Edwards, R.L., Sinha, A., Spötl, C., Yi, L., Chen, S., Kelly, M., Kathayat, G., Wang, X., Li, X., Kong, X., Wang, Y., Ning, Y., Zhang, H., 2016. The Asian monsoon over the past 640,000 years and ice age terminations. Nature. 534, 640–646.Clark, I., Fritz, P., 1997. Environmnetal Istopes in Hydrogeology. Lewis Publishers, New York.deMenocal, P.B., 1995. Plio-Pleistocene African Climate. Science. 270, 53–59.El-Shenawy, M.I., Kim, S.-T., Schwarcz, H.P., Asmerom, Y., Polyak, V.J., 2018. Speleothem evidence for the greening of the Sahara and its implications for the early human dispersal out of sub-Saharan Africa. Quaternary Science Reviews. 188, 67–76.Erlandson, J.M., Braje, T.J., 2015. Coasting out of Africa: The potential of mangrove forests and marine habitats to facilitate human coastal expansion via the Southern Dispersal Route. Quaternary International. 382, 31–41.Fick, S.E., Hijmans, R.J., 2017. WorldClim 2: new 1-km spatial resolution climate surfaces for global land areas. International Journal of Climatology. 37, 4302–4315.Fleitmann, D., 1997. Klastischer Eintrag in das Rote Meer und den Golf von Aden durch den Arabischen Monsun-Untersuchungen an Kolbenlot-Kernen. Diplom-Arbeit, Institut und Museum für Geologie und Paläontologie der Georg-August-Universität zu Göttingen.Fleitmann, D., Burns, S.J., Mangini, A., Mudelsee, M., Kramers, J., Villa, I., Neff, U., Al-Subbary, A.A., Buettner, A., Hippler, D., Matter, A., 2007. Holocene ITCZ and Indian monsoon dynamics recorded in stalagmites from Oman and Yemen (Socotra). Quaternary Science Reviews. 26, 170–188.Fleitmann, D., Burns, S.J., Mudelsee, M., Neff, U., Kramers, J., Mangini, A., Matter, A., 2003a. Holocene forcing of the Indian monsoon recorded in a stalagmite from Southern Oman. Science. 300, 1737–1739.Fleitmann, D., Burns, S.J., Neff, U., Mangini, A., Matter, A., 2003b. Changing moisture sources over the last 330,000 years in Northern Oman from fluid-inclusion evidence in speleothems. Quaternary Research. 60, 223–232.Fleitmann, D., Burns, S.J., Neff, U., Mudelsee, M., Mangini, A., Matter, A., 2004. Palaeoclimatic interpretation of high-resolution oxygen isotope profiles derived from annually laminated speleothems from Southern Oman. Quaternary Science Reviews. 23, 935–945.Fleitmann, D., Burns, S.J., Pekala, M., Mangini, A., Al-Subbary, A., Al-Aowah, M., Kramers, J., Matter, A., 2011. Holocene and Pleistocene pluvial periods in Yemen, southern Arabia. Quaternary Science Reviews. 30, 783–787.GEBCO Compilation Group, 2020. GEBCO 2020 Grid.Gierz, P., Werner, M., Lohmann, G., 2017. Simulating climate and stable water isotopes during the Last Interglacial using a coupled climate-isotope model. Journal of Advances in Modeling Earth Systems. 9, 2027–2045.Grant, K.M., Grimm, R., Mikolajewicz, U., Marino, G., Ziegler, M., Rohling, E.J., 2016. The timing of Mediterranean sapropel deposition relative to insolation, sea-level and African monsoon changes. Quaternary Science Reviews. 140, 125–141.Grant, K.M., Rohling, E.J., Bar-Matthews, M., Ayalon, A., Medina-Elizalde, M., Ramsey, C.B., Satow, C., Roberts, A.P., 2012. Rapid coupling between ice volume and polar temperature over the past 50,000 years. Nature. 491, 744–747.Grant, K.M., Rohling, E.J., Ramsey, C.B., Cheng, H., Edwards, R.L., Florindo, F., Heslop, D., Marra, F., Roberts, A.P., Tamisiea, M.E., Williams, F., 2014. Sea-level variability over five glacial cycles. Nature Communications. 5, 5076.Grant, K.M., Rohling, E.J., Westerhold, T., Zabel, M., Heslop, D., Konijnendijk, T., Lourens, L., 2017. A 3 million year index for North African humidity/aridity and the implication of potential pan-African Humid periods. Quaternary Science Reviews. 171, 100–118.Groucutt, H.S., 2020. Volcanism and human prehistory in Arabia. Journal of Volcanology and Geothermal Research. 402, 107003.Groucutt, H.S., Petraglia, M.D., Bailey, G., Scerri, E.M.L., Parton, A., Clark-Balzan, L., Jennings, R.P., Lewis, L., Blinkhorn, J., Drake, N.A., Breeze, P.S., Inglis, R.H., Devès, M.H., Meredith-Williams, M., Boivin, N., Thomas, M.G., Scally, A., 2015a. Rethinking the dispersal of Homo sapiens out of Africa. Evolutionary Anthropology. 24, 149–164.Groucutt, H.S., Scerri, E.M.L., Lewis, L., Clark-Balzan, L., Blinkhorn, J., Jennings, R.P., Parton, A., Petraglia, M.D., 2015b. Stone tool assemblages and models for the dispersal of Homo sapiens out of Africa. Quaternary International. 382, 8–30.Groucutt, H.S., Scerri, E.M.L., Stringer, C., Petraglia, M.D., 2019. Skhul lithic technology and the dispersal of Homo sapiens into Southwest Asia. Quaternary International. 515, 30–52.Groucutt, H.S., White, T.S., Clark-Balzan, L., Parton, A., Crassard, R., Shipton, C., Jennings, R.P., Parker, A.G., Breeze, P.S., Scerri, E.M.L., Alsharekh, A., Petraglia, M.D., 2015c. Human occupation of the Arabian Empty Quarter during MIS 5: Evidence from Mundafan Al-Buhayrah, Saudi Arabia. Quaternary Science Reviews. 119, 116–135.Häuselmann, A.D., Fleitmann, D., Cheng, H., Tabersky, D., Günther, D., Edwards, R.L., 2015. Timing and nature of the penultimate deglaciation in a high alpine stalagmite from Switzerland. Quaternary Science Reviews. 126, 264–275.Herold, M., Lohmann, G., 2009. Eemian tropical and subtropical African moisture transport: An isotope modelling study. Climate Dynamics. 33, 1075–1088.Jennings, R.P., Shipton, C., Breeze, P., Cuthbertson, P., Bernal, M.A., Wedage, W.M.C.O., Drake, N.A., White, T.S., Groucutt, H.S., Parton, A., Clark-Balzan, L., Stimpson, C., al Omari, A.A., Alsharekh, A., Petraglia, M.D., 2015. Multi-scale Acheulean landscape survey in the Arabian Desert. Quaternary International. 382, 58–81.Lamb, H.F., Bates, C.R., Bryant, C.L., Davies, S.J., Huws, D.G., Marshall, M.H., Roberts, H.M., 2018. 150,000-year palaeoclimate record from northern Ethiopia supports early, multiple dispersals of modern humans from Africa. Scientific Reports. 8.Larrasoaña, J.C., Roberts, A.P., Rohling, E.J., 2013. Dynamics of Green Sahara Periods and Their Role in Hominin Evolution. PLoS ONE. 8, e76514.Larrasoana, J.C., Roberts, A.P., Rohling, E.J., Winklhofer, M., Wehausen, R., 2003. Three million years of monsoon variability over the northern Sahara. Climate Dynamics. 21, 689–698.Lisiecki, L.E., Raymo, M.E., 2005. A Pliocene-Pleistocene stack of 57 globally distributed benthic 18O records. Paleoceanography. 20, 1–17.\Marino, G., Rohling, E.J., Rodríguez-Sanz, L., Grant, K.M., Heslop, D., Roberts, A.P., Stanford, J.D., Yu, J., 2015. Bipolar seesaw control on last interglacial sea level. Nature. 522, 197–201.McLaren, S.J., Al-Juaidi, F., Bateman, M.D., Millington, A.C., 2009. First evidence for episodic flooding events in the arid interior of central Saudi Arabia over the last 60 ka. Journal of Quaternary Science. 24, 198–207.Mellars, P., Gori, K.C., Carr, M., Soares, P.A., Richards, M.B., 2013. Genetic and archaeological perspectives on the initial modern human colonization of southern Asia. Proceedings of the National Academy of Sciences. 110, 10699–10704.Millard, A.R., 2008. A critique of the chronometric evidence for hominid fossils: I. Africa and the Near East 500-50 ka. Journal of Human Evolution. 54, 848–847.Nicholson, S.L., Hosfield, R., Groucutt, H.S., Pike, A.W.G., Fleitmann, D., 2021. Beyond arrows on a map: The dynamics of Homo sapiens dispersal and occupation of Arabia during Marine Isotope Stage 5. Journal of Anthropological Archaeology. 62, 101269.Nicholson, S.L., Pike, A.W.G., Hosfield, R., Roberts, N., Sahy, D., Woodhead, J., Cheng, H., Edwards, R.L., Affolter, S., Leuenberger, M., Burns, S.J., Matter, A., Fleitmann, D., 2020. Pluvial periods in Southern Arabia over the last 1.1 million-years. Quaternary Science Reviews. 229, 106112.Norman, K., Inglis, J., Clarkson, C., Faith, J.T., Shulmeister, J., Harris, D., 2018. An early colonisation pathway into northwest Australia 70-60,000 years ago. Quaternary Science Reviews. 180, 229–239.Otto-Bliesner, B.L., 2006. Simulating Arctic Climate Warmth and Icefield Retreat in the Last Interglaciation. Science. 311, 1751–1753.Parton, A., Clark-Balzan, L., Parker, A.G., Preston, G.W., Sung, W.W., Breeze, P.S., Leng, M.J., Groucutt, H.S., White, T.S., Alsharekh, A., Petraglia, M.D., 2018. Middle-late quaternary palaeoclimate variability from lake and wetland deposits in the Nefud Desert, Northern Arabia. Quaternary Science Reviews. 202, 78–97.Parton, A., Farrant, A.R., Leng, M.J., Schwenninger, J.L., Rose, J.I., Uerpmann, H.P., Parker, A.G., 2013. An early MIS 3 pluvial phase in Southeast Arabia: Climatic and archaeological implications. Quaternary International. 300, 62–74.Parton, A., Farrant, A.R., Leng, M.J., Telfer, M.W., Groucutt, H.S., Petraglia, M.D., Parker, A.G., 2015. Alluvial fan records from southeast Arabia reveal multiple windows for human dispersal. Geology. 43, 295–298.Petit-Maire, N., Carbonel, P., Reyss, J.L., Sanlaville, P., Abed, A.M., Bourrouilh, R., Fontugne, M.R., Yasin, S., 2010. A vast Eemian palaeolake in Southern Jordan (29°N). Global and Planetary Change. 72, 368–373.Petraglia, M.D., Alsharekh, A., Breeze, P., Clarkson, C., Crassard, R., Drake, N.A., Groucutt, H.S., Jennings, R.P., Parker, A.G., Parton, A., Roberts, R.G., Shipton, C., Matheson, C., Al-Omari, A., Veall, M.A., 2012. Hominin Dispersal into the Nefud Desert and Middle Palaeolithic Settlement along the Jubbah Palaeolake, Northern Arabia. PLoS ONE. 7, e49840.Petraglia, M.D., Alsharekh, A.M., Crassard, R., Drake, N.A., Groucutt, H., Parker, A.G., Roberts, R.G., 2011. Middle Paleolithic occupation on a Marine Isotope Stage 5 lakeshore in the Nefud Desert, Saudi Arabia. Quaternary Science Reviews. 30, 1555–1559.Petraglia, M.D., Breeze, P.S., Groucutt, H.S., 2019. Blue Arabia, Green Arabia: Examining Human Colonisation and Dispersal Models. In: Rasul, N.M.A., Stewart, I.C.F. (Eds.), Geological Setting, Palaeoenvironment and Archaeology of the Red Sea. Springer International Publishing, Cham, pp. 675–683.Petraglia, M.D., Parton, A., Groucutt, H.S., Alsharekh, A., 2015. Green Arabia: Human prehistory at the Crossroads of Continents. Quaternary International. 382, 1–7.Rohling, E.J., Grant, K., Bolshaw, M., Roberts, A.P., Siddall, M., Hemleben, C., Kucera, M., 2009. Antarctic temperature and global sea level closely coupled over the past five glacial cycles. Nature Geoscience. 2, 500–504.Rohling, E.J., Grant, K.M., Roberts, A.P., Larrasoaña, J.-C., 2013. Paleoclimate Variability in the Mediterranean and Red Sea Regions during the Last 500,000 Years. Current Anthropology. 54, S183–S201.Rohling, E.J., Marino, G., Grant, K.M., 2015. Mediterranean climate and oceanography, and the periodic development of anoxic events (sapropels). Earth-Science Reviews. 143, 62–97.Rose, J.I., Usik, V.I., Marks, A.E., Hilbert, Y.H., Galletti, C.S., Parton, A., Geiling, J.M., Černý, V., Morley, M.W., Roberts, R.G., 2011. The Nubian complex of Dhofar, Oman: An African Middle Stone Age industry in Southern Arabia. PLoS ONE. 6, e28239.Rosenberg, T.M., Preusser, F., Blechschmidt, I., Fleitmann, D., Jagher, R., Matter, A., 2012. Late Pleistocene palaeolake in the interior of Oman: A potential key area for the dispersal of anatomically modern humans out-of-Africa? Journal of Quaternary Science. 27, 13–16.Rosenberg, T.M., Preusser, F., Fleitmann, D., Schwalb, A., Penkman, K.E.H., Schmid, T.W., Al-Shanti, M.A., Kadi, K.A., Matter, A., 2011. Humid periods in southern Arabia: Windows of opportunity for modern human dispersal. Geology. 39, 1115–1118.Rosenberg, T.M., Preusser, F., Risberg, J., Plikk, A., Kadi, K.A., Matter, A., Fleitmann, D., 2013. Middle and Late Pleistocene humid periods recorded in palaeolake deposits of the Nafud desert, Saudi Arabia. Quaternary Science Reviews. 70, 109–123.Siddall, M., Rohling, E.J., Almogi-Labin, A., Hemleben, C., Meischner, D., Schmelzer, I., Smeed, D.A., 2003. Sea-level fluctuations during the last glacial cycle. Nature. 423, 853–858.Stewart, M., Clark-Wilson, R., Breeze, P.S., Janulis, K., Candy, I., Armitage, S.J., Ryves, D.B., Louys, J., Duval, M., Price, G.J., Cuthbertson, P., Bernal, M.A., Drake, N.A., Alsharekh, A.M., Zahrani, B., Al-Omari, A., Roberts, P., Groucutt, H.S., Petraglia, M.D., 2020a. Human footprints provide snapshot of last interglacial ecology in the Arabian interior. Science Advances. 6, eaba8940.Stewart, M., Louys, J., Breeze, P.S., Clark-Wilson, R., Drake, N.A., Scerri, E.M.L., Zalmout, I.S., Al-Mufarreh, Y.S.A., Soubhi, S.A., Haptari, M.A., Alsharekh, A.M., Groucutt, H.S., Petraglia, M.D., 2020b. A taxonomic and taphonomic study of Pleistocene fossil deposits from the western Nefud Desert, Saudi Arabia. Quaternary Research. 95, 1–22.Tierney, J.E., deMenocal, P.B., Zander, P.D., 2017. A climatic context for the out-of-Africa migration. Geology. 45, 1023–1026.Torfstein, A., Goldstein, S.L., Kushnir, Y., Enzel, Y., Haug, G., Stein, M., 2015. Dead Sea drawdown and monsoonal impacts in the Levant during the last interglacial. Earth and Planetary Science Letters. 412, 235–244.Vaks, A., Bar-Matthews, M., Ayalon, A., Matthews, A., Frumkin, A., Dayan, U., Halicz, L., Almogi-Labin, A., Schilman, B., 2006. Paleoclimate and location of the border between Mediterranean climate region and the Saharo-Arabian Desert as revealed by speleothems from the northern Negev Desert, Israel. Earth and Planetary Science Letters. 249, 384–399.Vaks, A., Bar-Matthews, M., Matthews, A., Ayalon, A., Frumkin, A., 2010. Middle-Late Quaternary paleoclimate of northern margins of the Saharan-Arabian Desert: Reconstruction from speleothems of Negev Desert, Israel. Quaternary Science Reviews. 29, 2647–2662.Weldeab, S., Lea, D.W., Schneider, R.R., Andersen, N., 2007. Supporting Online Material for 155,000 Years of West African Monsoon and Ocean Thermal Evolution. Science. 316, 0–9.

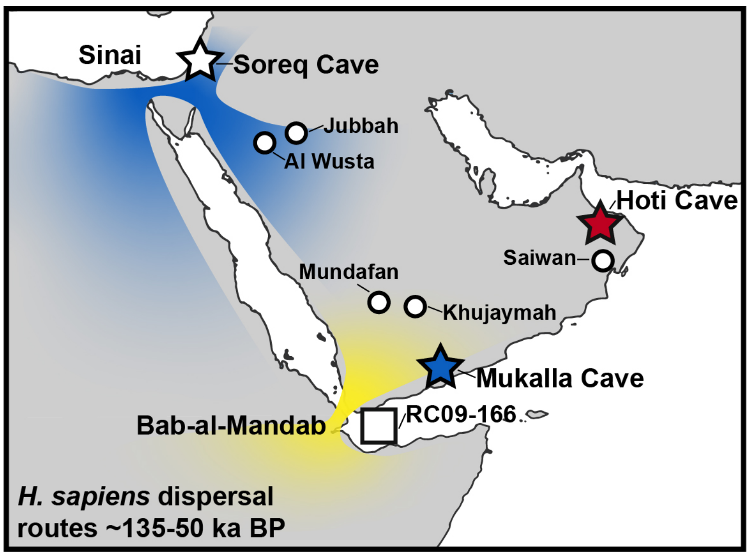

Fig. 1. Map of Arabia with locations of Mukalla Cave (blue star), Hoti Cave (red star), Soreq Cave (white star), palaeolakes (white circles), RC09-166 (white square) and proposed *H. sapiens* northern (blue) and southern (yellow) entry points into Arabia (Armitage et al., 2011; Rohling et al., 2013; Petraglia et al., 2019).

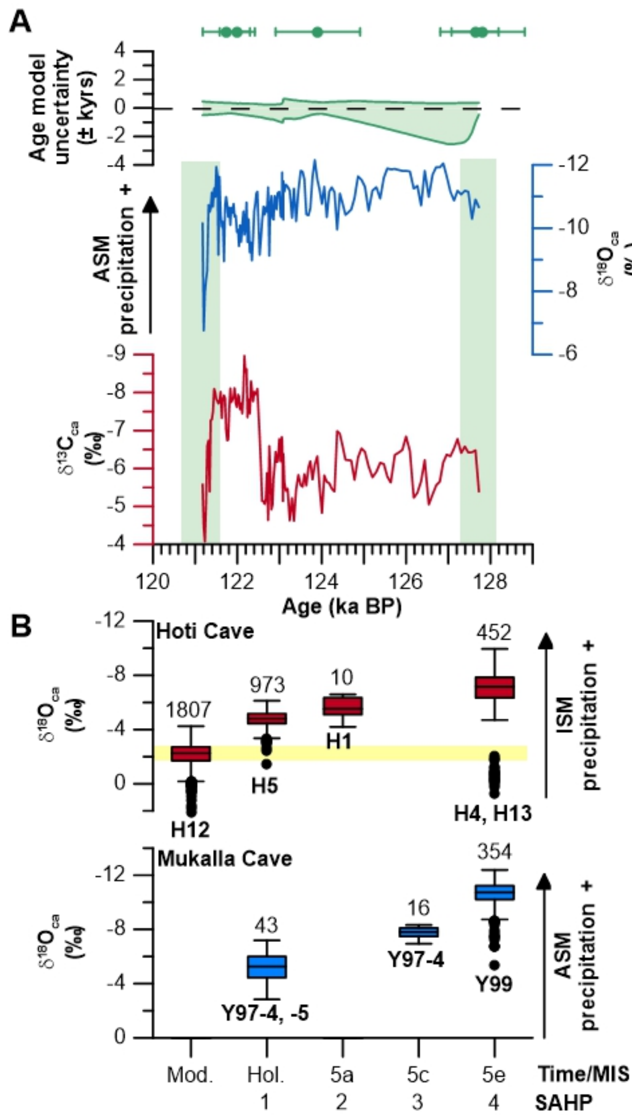

Fig. 2. A) ^{230}Th ages, StalAge model uncertainty, $^{18}O_{ca}$ and $^{13}C_{ca}$ values of GI-I (MIS 5e) of Y99. B) Box-whisker plot comparison of Hoti Cave (Oman) and Mukalla Cave (Yemen) stalagmite $^{18}O_{ca}$ values from Fleitmann et al. (2011) and Nicholson et al. (2020). Numbers above and below box-whiskers indicate amount of $^{18}O_{ca}$ measurements and speleothem samples, respectively. The yellow bar denotes the range of modern ^{18}O values in Oman, derived mostly from winter rainfall.

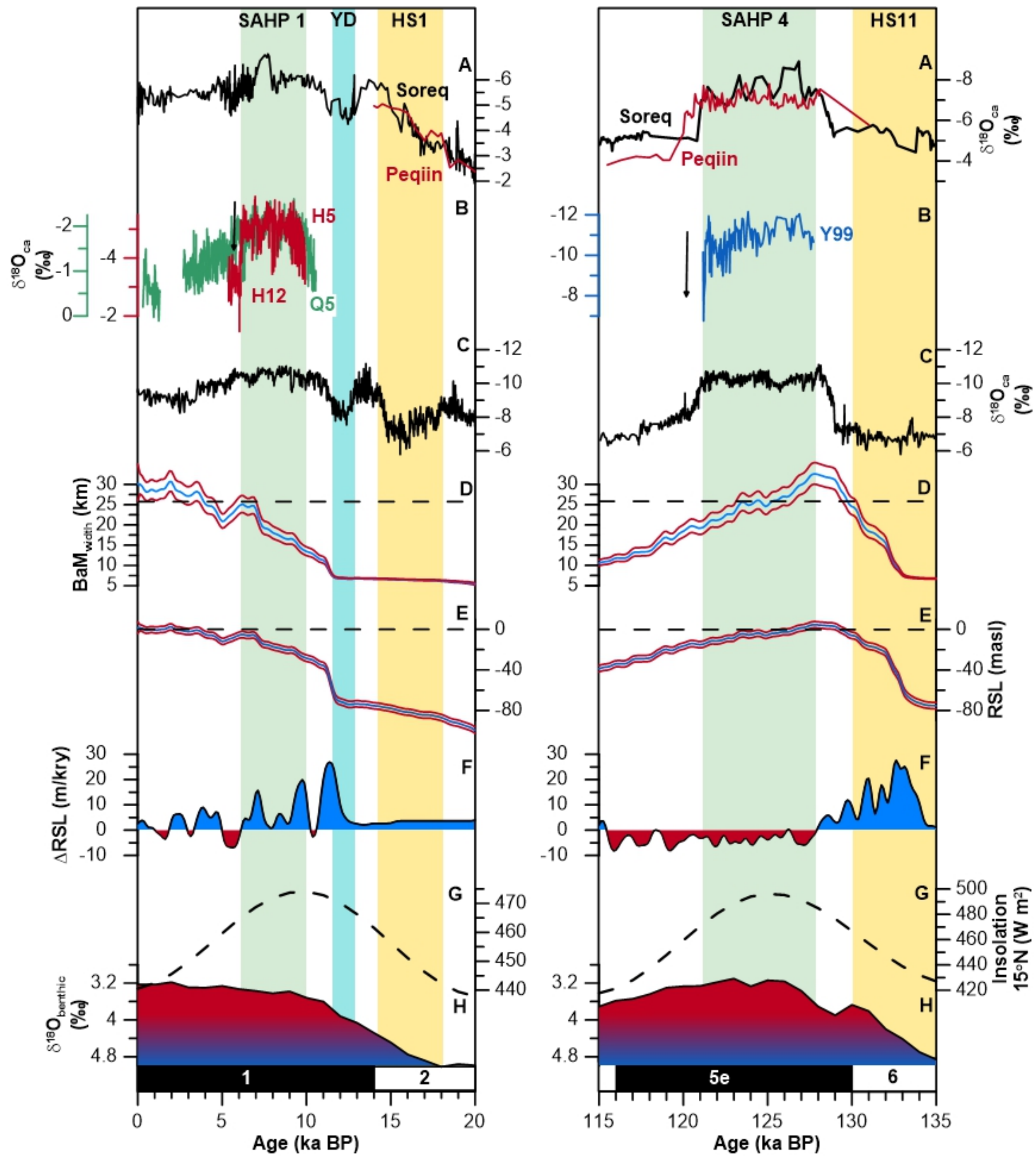

Fig. 3. (A) Soreq and Peqiin cave $^{18}O_{ca}$. (B) Holocene (H5, H12 and Q5) and MIS 5e (Y99) stalagmite $^{18}O_{ca}$ records from Qunf Cave (green) (Fleitmann et al., 2003a), Hoti Cave (red) (Fleitmann et al., 2004, 2007) and Mukalla Cave (blue). (C) Sanbao Cave (China) composite stalagmite $^{18}O_{ca}$ (Cheng et al.,

2009, 2016). (D) Reconstructed Bab-al-Mandab width using bathymetry data (GEBCO) and (E) the Relative sea-level (RSL) curve Probability-Maximum (blue), 95% confidence intervals (red) (Grant et al., 2012, 2014). (F) Rate of sea-level change predicted from RSL (Grant et al., 2012, 2014). (G) July insolation (W m_2) at 15°N (Berger and Loutre, 1991, 1999). (H) Global ice-volume (LR04 $^{18}O_{benthic}$) and Marine Isotope Stages (Lisiecki and Raymo, 2005). Green bars denote duration of SAHP 1 and 4, yellow bars denote timing of Heinrich Stadial 1 and 11 and the blue bar denotes the timing of the Younger Dryas event.

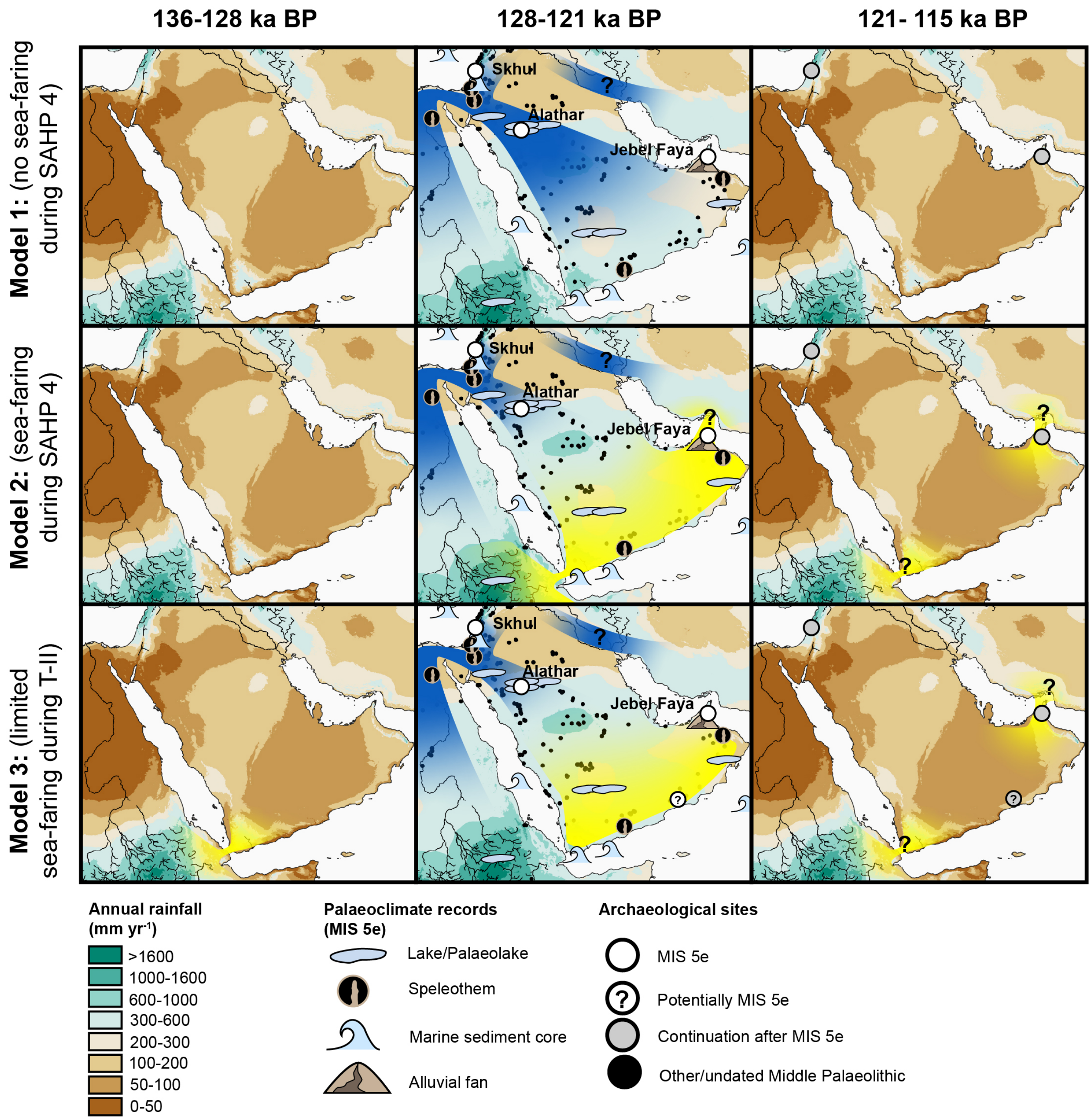

Fig. 4. Conceptual illustration of models for *H. sapiens* populations dispersals between 135-121 ka BP over northern (blue) and southern (yellow) routes. Rainfall maps include simulations for 140-120 ka BP (Otto-Bliesner, 2006) and the present-day (Fick and Hijmans, 2017) and are tuned to the chronology of Y99. All three models assume that the Sinai Peninsula (northern-route) was

also a likely entry point into Arabia (supported by the assessment of archaeological assemblages from NE Africa, the Levant and northern Arabia). MIS 5e archaeological sites include the Alathar footprints (Saudi Arabia; Stewart et al., 2020b), Jebel Faya (Oman; Armitage et al., 2011), Skhul (Israel; Millard, 2008) and possibly Aybut al Awal (Oman; Rose et al., 2011). Undated/other Middle Palaeolithic sites were collated from (Groucutt et al., 2015b). Palaeoclimate records showing evidence of increased regional rainfall during MIS 5e include Mukalla Cave (Yemen; this study), Hoti Cave (Oman; Burns et al., 2001; Fleitmann et al., 2003; 2011), Soreq Cave and Negev Desert caves (Israel; Bar-Matthews et al., 2003; Vaks et al., 2006; 2010) and Wadi-Sannur Cave (Egypt; El-Shenawy et al., 2018) stalagmites; Palaeolakes Mundafan, Khujaymah, Jubbah, Alathar, Khall Amaysham, B'r Hayzan and Ti's al Ghada (Saudi Arabia; Petraglia et al., 2011; 2012; Rosenberg et al., 2011; 2013; Stewart et al., 2020b), Saiwan (Oman; Rosenberg et al., 2012), Lake Tana (Ethiopia; Lamb et al., 2018), and Mudawwara (Jordan; Petit-Maire et al., 2010); Marine records KL-15 and RC09-166 (Gulf of Aden; Fleitmann, 1997; Tierney et al., 2017), ODP 721/722 (Arabian Sea; deMenocal, 1995), KL-11 (Red Sea; Fleitmann, 1997; Siddall et al., 2003); ODP 967 (Mediterranean Sea; Larrasoana et al., 2003; Grant et al., 2017), and DSDDP (Dead Sea; Torfstein et al., 2015).